EVALUATION OF REPAIR EFFECT FOR DETERIORATED CONCRETE PIERS OF INTAKE DAM USING AE ACTIVITY

TOMOKI SHIOTANI and DIMITRIOS G. AGGELIS*

Department of Urban Management, Graduate School of Engineering, Kyoto University, C1-2-236, Kyoto-Daigaku-Katsura, Nishikyo, Kyoto 615-8540, Japan; *Research Institute of Technology, Tobishima Corporation, 5472 Kimagase, Noda, Chiba, 270-0222, Japan

Abstract

Deteriorated concrete structures are repaired by means of grouting. In order to evaluate the repair effectiveness, the application of two NDT techniques, namely seismic tomography and acoustic emission is described herein. Using the traveling time of elastic waves, the structural velocity is estimated. AE activity is monitored along with water pressurization of the permeability test. As a result, contrary to the common expectation that the velocity increases after filling with grouting agent, enormous amount of velocity drop was observed after repair, due to the incomplete hydration process of grout material and the resulting property mis-match. On the other hand, AE activity showed dramatic decrease after repair. Furthermore, the results are correlated to the quantity of grouting material injected, showing that this was the source of the velocity behavior, while it became clear that damage indices based on AE activity exhibited well the actual damage of concrete structures.

Keywords: Damage indices, deterioration, concrete structures, tomography, repair effect

Introduction

The present paper reports on the repair evaluation of a water intake diversion facility that was constructed 70 years ago in a cold region of Japan. The concrete piers, which support the rolling gate, the most crucial part of the facility, exhibited deterioration. Referring to the repair record of the facility, both sides of the pier were replaced to the depth of 20 cm with new concrete 20 years ago, since macroscopic surface cracks developed resulting from freezing and thawing. Recently, the surface degradation became critical again; therefore damage investigation was performed by means of core sampling. Two seriously damaged zones were observed: at the boundary between the old and the replaced concrete, and in the deep, internal area of the pier owing to a large amount of voids, pieces of wood and cobblestone. Grouting with injection cement was used for repair and the present paper describes the applicability of NDT to evaluate the repair effectiveness.

Experimental

Repair Technique

The concrete piers described herein are referenced as Pier 1 and Pier 2. Two directions of grouting were used: (i) vertical grouting to fill the internal damaged areas, (ii) horizontal grouting to fill the interface between the old and replaced concrete along both sides. Specifically, a vertical borehole with 50-mm diameter was drilled only for Pier 1, whereas many horizontal boreholes with 20-mm diameter from both bank sides (only to shallow depth ranging from 800 to 1000 mm) were made in both piers. The arrangement of the boreholes can be seen in Fig. 1.

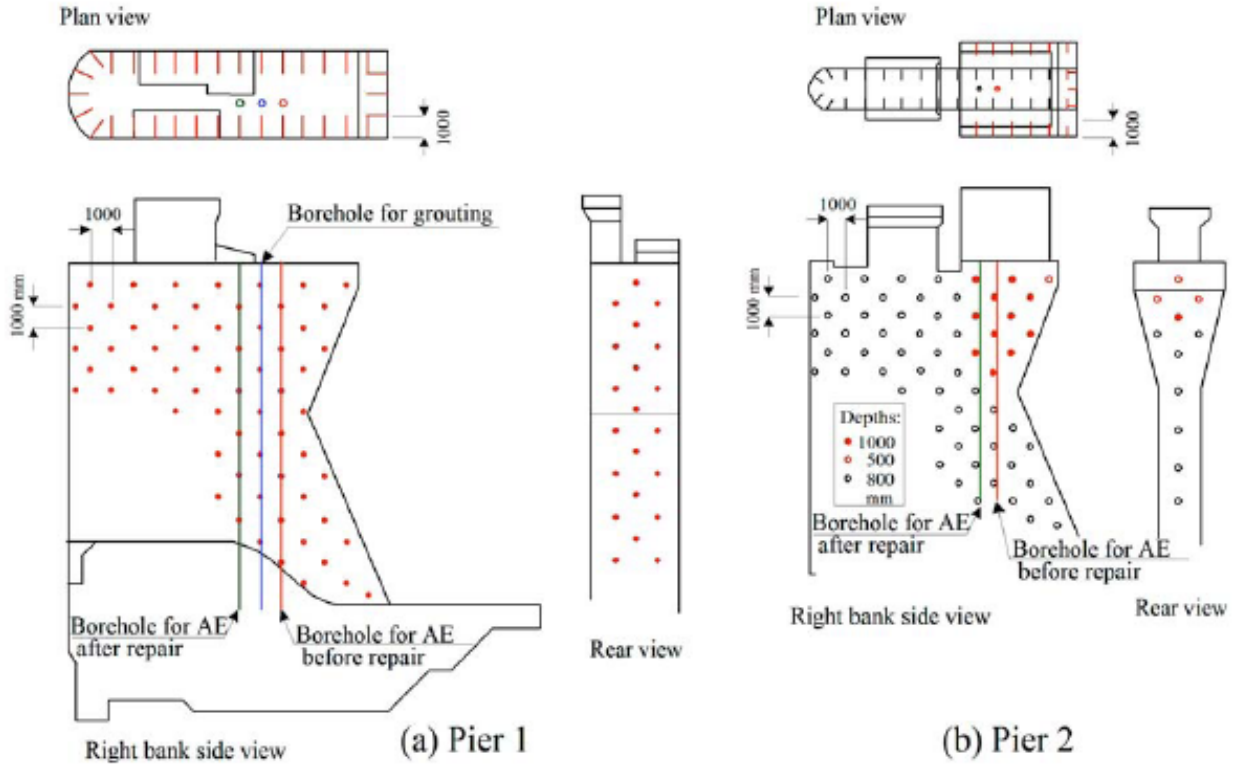

Fig. 1 (a) Grouting maps for Pier 1; (b) Pier 2.

NDT Monitoring

In order to verify the repair effectiveness before and after repair, seismic tomography and acoustic emission (AE) were performed. Through seismic tomography, the velocity structure can be created from P-wave traveling time. The velocity difference between before and after repair leads to the characterization of the repair (Shiotani et al., 2005a). Using AE activity, damage can also be quantified with indices such as RTRI and Calm ratio (Luo et al., 2004), and even in cases when those are difficult to apply, AE peak amplitude distribution can give reasonable evaluation of the damage extent (Shiotani et al., 2005b).

Seismic Tomography

Seismic tomography needs both excitation and detection of elastic waves. They were performed with a hammer drill edged with different curvatures of 10, 20 and 30 mm in radius and piezoelectric accelerometers (SAF51, Fuji Ceramics Corp.). The curvature was altered to examine the relation between resulted velocities and the upper range of excited elastic wave frequency (Sansalone & Street, 1997). The present paper only shows the result of 30 mm in radius (others can be seen in Shiotani and Aggelis, 2006). Figure 2 shows the arrangement of accelerometers in Pier 1 used for tomography. 16 channels of accelerometers were used, one of which acted as a trigger sensor and 15 others as receivers. The receivers are placed in a vertical line, with equal space of 500 mm on one lateral side, while on the opposite side excitation was performed by a hammer drill, with a near-by trigger accelerometer. The hammering was continuously excited for 10 seconds with 30 Hz repetition, resulting in about 300 waveforms. Using the 300 waveforms, stacking was conducted to enhance the signal-to-noise ratio and to facilitate the first-arrival picking. The traveling time was fed to a suitable tomography program (see Kobayashi et al., 2006). Using seismic tomography the velocity structure of the pier was reconstructed in two different cross-sections, namely upper current section and lower current section (see Fig. 2).

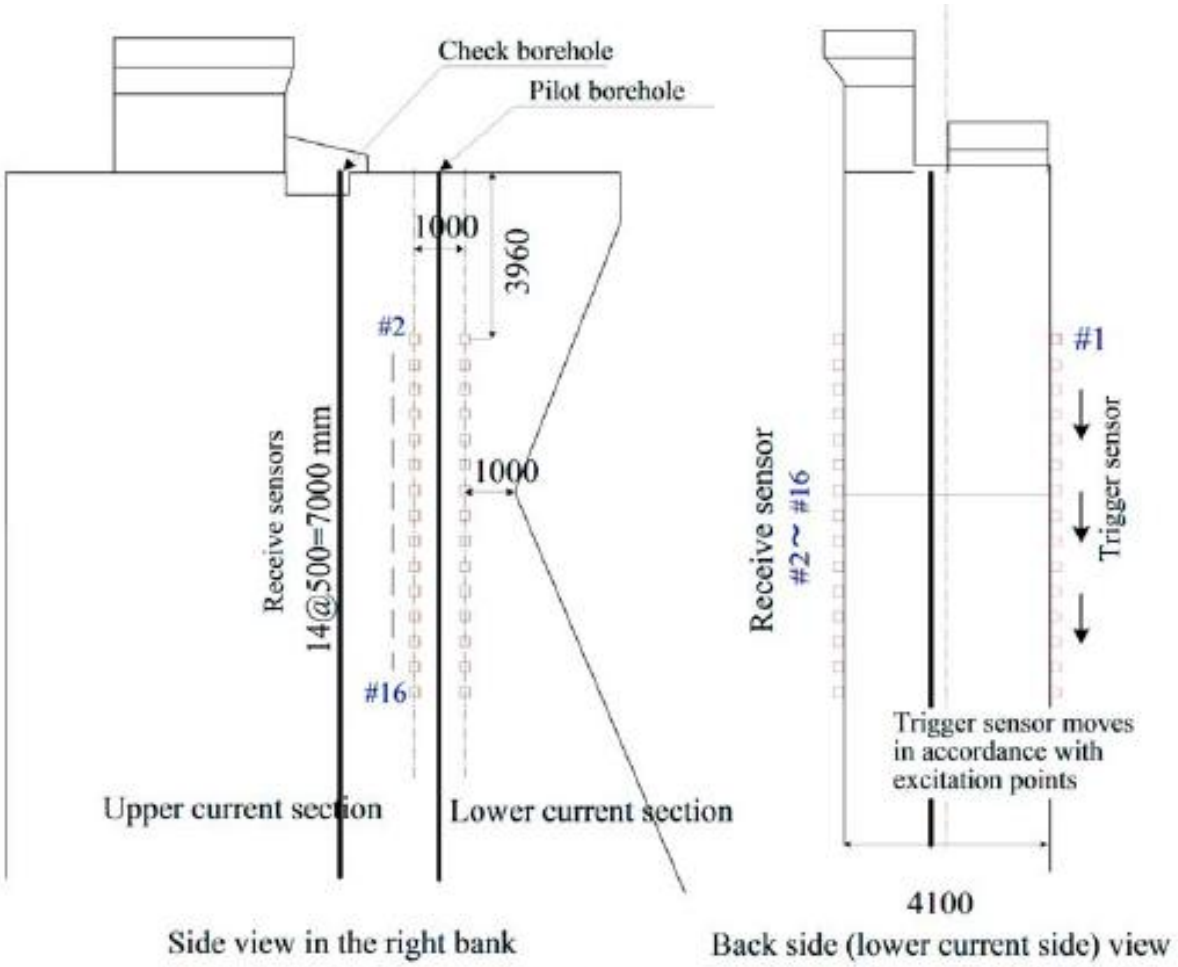

Fig. 2 Sensor array for tomography in Pier 1.

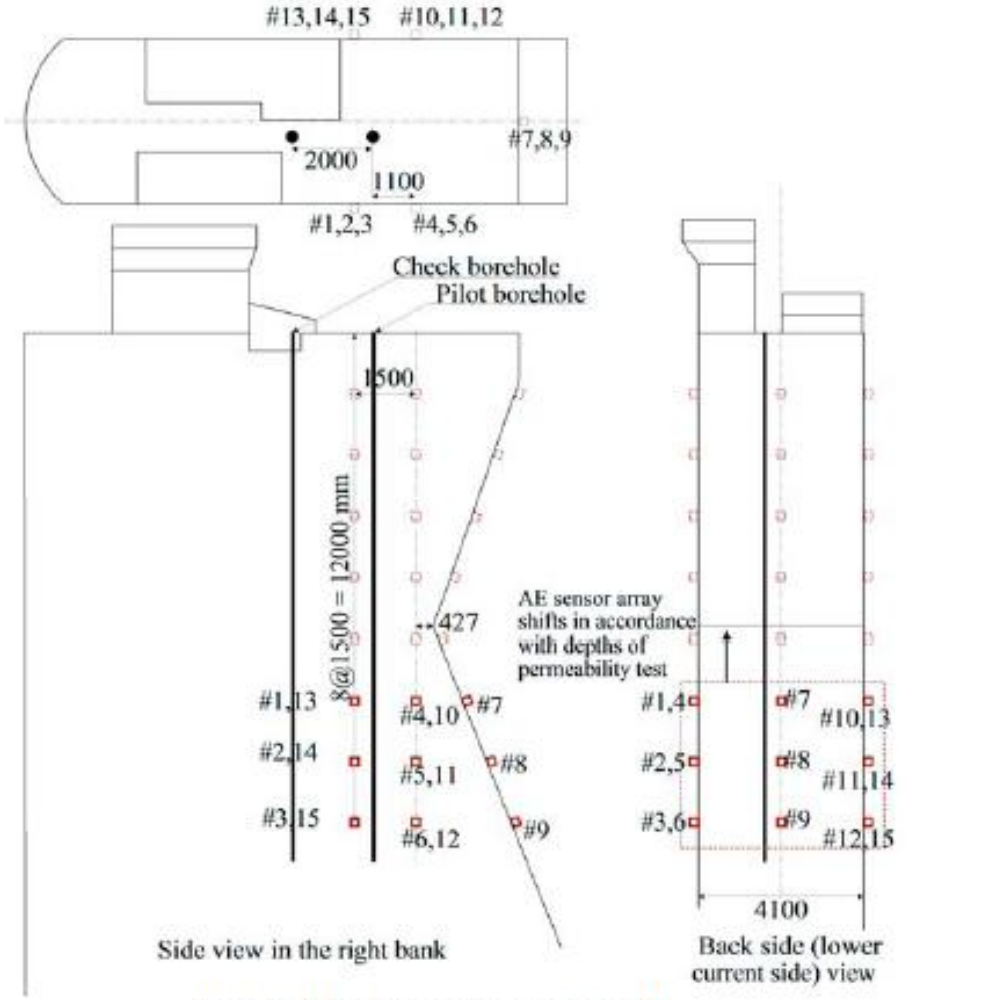

Fig. 3 AE sensor array in Pier 1.

Acoustic Emission

To study if the grouting material filled the cracked or void areas, permeability tests were carried out by means of a water pump. AE monitoring was conducted during the application of water pressure. As shown in Fig. 3, 6 sensors on each side and 3 sensors on the back side were set with 1.5-m spacing, making a total of 15 sensors. The permeability of concrete was monitored in intervals of 1 m in depth, together with AE monitoring. The AE signals detected with AE sensors (R6I, PAC) were amplified 40 dB and the signals over 40 dB were acquired by DISP AE system (PAC) to study their AE parameters as well as waveforms.

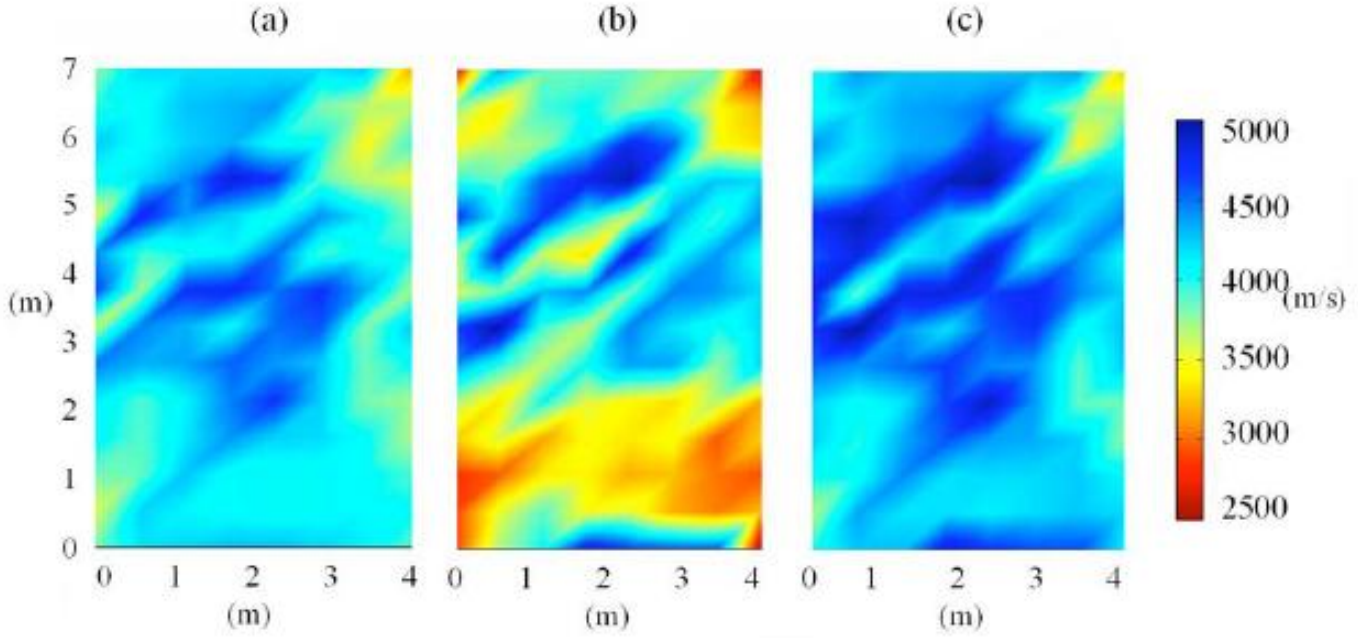

Fig. 4 Tomogram of a dam pier section examined (a) before, (b) after repair, (c) after complete hardening of grout.

Results

Seismic Tomography

In Fig. 4(a) the tomogram of a cross section of Pier 1 before injection of grout is presented. The general condition can be characterized satisfactory since the propagation velocity is generally higher than 3500 m/s, except in some small areas. However, two weeks after repair, the tomogram showed clearly decreased velocity, even as low as 2500 m/s (see Fig. 4(b)). This behavior was not expected since cementitious material replaced the voids. Even if the defects were not completely eliminated, the velocity was not supposed to decrease.

Since grouted concrete is a highly heterogeneous medium, it was deemed essential to investigate stress wave scattering, which is known to produce strong dispersive effects (Tsinopoulos et al., 2000). The model studied was that of an elastic concrete matrix initially containing voids (case before repair), subsequently soft elastic scatterers (shortly after repair) and finally hard elastic scatterers (fully hardened grout pockets). The properties of concrete were derived by cores from the dam, while concerning grout, specimens of the same material were created and tested in laboratory at different ages.

With the knowledge of mechanical properties of the constituent materials, the wavenumber of the composite can be calculated using a suitable dispersion relation (Waterman & Truell, 1961):

$$\left(\frac{k}{k_c}\right)^2 = 1 + \frac{3\varphi}{k_c^2 R^3} f(0) + \frac{9\varphi^2}{4k_c^4 R^6}\left[f^2(0) - f^2(\pi)\right] \quad (1)$$

where R is the scatterer radius (in this case void or grout pocket), φ is the particle volume concentration, k_c the wavenumber of the matrix and f(0) and f(π) are the forward and backward far-field scattering amplitudes, respectively, showing what part of energy is scattered forward and backward (Ying and Truell, 1956).

The frequency dependent phase velocity C(ω) and attenuation α(ω) are calculated from the complex wavenumber of the medium:

$$k(\omega) = \frac{\omega}{C(\omega)} + i\alpha(\omega) \quad (2)$$

where ω stands for radial frequency.

The characteristic size of the voids is not readily known. However, due to the low sonic frequencies excited at the test, wavelengths of typically 0.5 m are employed, which are certainly larger than most cracks present in the material. Therefore, the size of scatterer is not crucial in our investigation. Assuming for example, void size of 40 mm, and void content of 15%, which is typical in literature (Chaix et al., 2006) and frequency 10 kHz, after solution of Eq. (1), the pulse velocity for concrete is calculated at 4300 m/s. If instead of voids, 15% of soft grout of 12 GPa is applied (corresponding to the elasticity of grout at the age of two weeks), the velocity reduces to 3850 m/s. Therefore, the scattering theory suggests that a velocity increase should not be expected immediately, but only after sufficient hardening of grout. This could be further delayed in a cold environment. For the final case of hardened grout of 22 GPa, the velocity increases to 4400 m/s (Aggelis & Shiotani, 2006a, 2006b). Using Eq. (1), since the mechanical properties of the materials have been determined and the velocities measured, the volume fraction of voids is calculated. This is done for each specific tomography cell, corresponding to an area of 0.5 x 0.5 m, for which velocity values have been assigned by tomography. In order to calculate the final velocity structure, which should be anticipated after full hydration of grout, the elasticity of 22 GPa is applied to Eq. (1), along with the corresponding void volume of each cell. Therefore, the final velocity structure is depicted in Fig. 4(c). The average velocity is increased by approximately 100 m/s, something that was not revealed by the monitoring just after the repair. However, using scattering theory, it was possible to explain the behavior and to evaluate the final condition of the structure.

According to the above discussion, the amount of grout is responsible for the initially observed velocity drop. This is confirmed by the correlation of the actual quantity of grout injected at different heights in the structure, with the velocity decrease at the same areas, depicted in Fig. 5. An excellent correlation is observed, since at the positions where a lot of grout was injected (e.g. 120 kg, 9 m from the top), at the same position, a velocity decrease of more than 800 m/s was measured.

Acoustic Emission

The source location algorithm failed to identify AE sources. Thus, the repair effect is discussed with AE hit activity. For Pier 1, Fig. 6a shows accumulated AE hits for each depth for the left bank side (right) and rear side (left). Especially for the left bank side, total AE hits of two allocated sensors at the same height are depicted with horizontal bars. In the chart, the injected quantity of vertical grout is drawn as well. Before repair, AE hit activity was intensively observed particularly below –9.0 m.

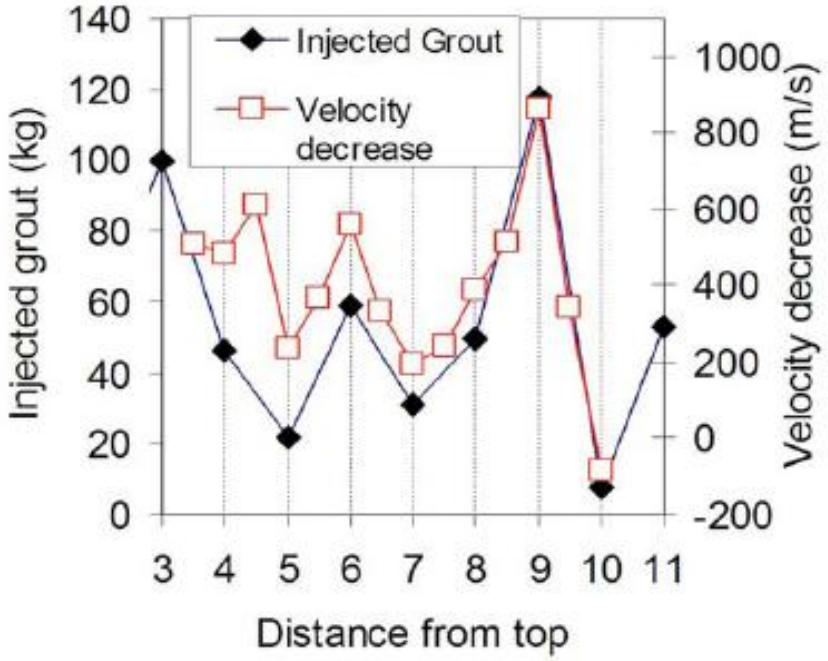

Fig. 5 Amount of grout and velocity decrease for different heights of pier 1.

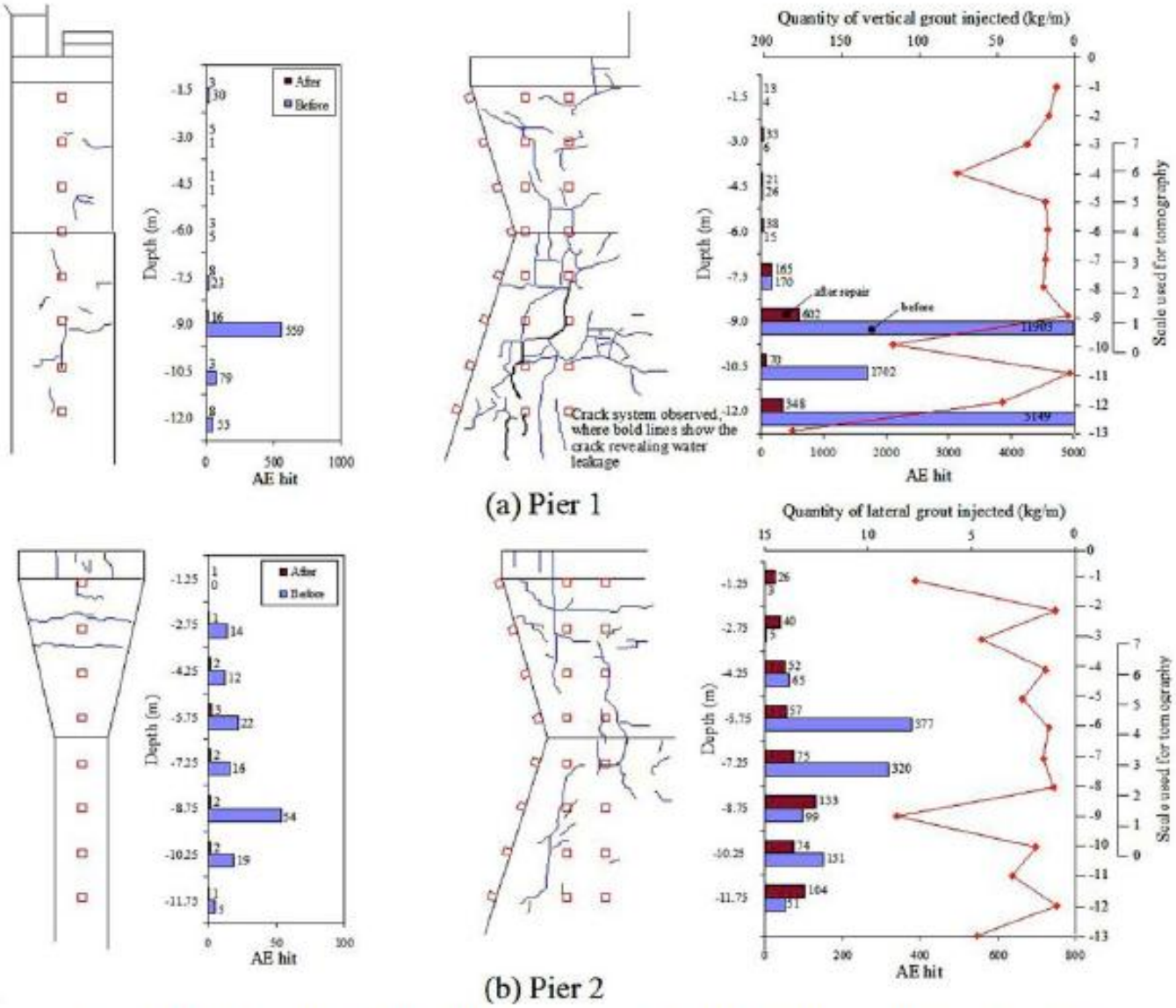

Fig. 6 AE hit activity with crack trace (Right: the left banks side, Left: rear side).

At these depths, a complicated and well-evolved surface crack system was observed, as well as water leakage from some macroscopic cracks among those (see bold lines in the figure), causing a large number of AE hits. A large amount of grout was injected vertically at those depths, implying that the macroscopic cracks were filled with the injection cement. AE activity after repair revealed decrease; i.e., from 5149 to 348 hits at –12 m and from 11903 to 602 hits at –9.0 m. The same trend could be found in the rear view (see the left graph in the figure) as AE hits decreased before and after repair.

The result for Pier 2 is shown in Fig. 6b. Steep changes of AE activity before and after repair were only derived around the middle height of monitoring range where 377 hits before repair decreased to 57 after at -5.75 m and 320 to 75 at -7.25 m (see the right chart in Fig. 6b). No correlation between the AE activity and the quantity of injected horizontal grout was observed.

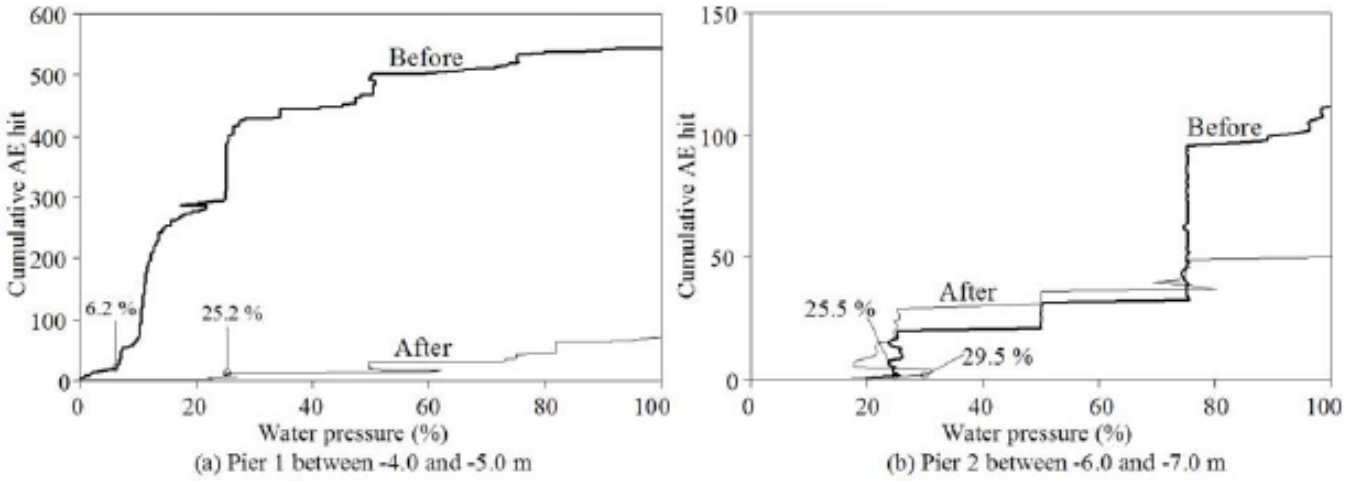

Fig. 7 AE hit activity with water pressurization process.

Hereafter, two damage indices namely Load ratio and Calm ratio are used to discuss the structural integrity. These indices are calculated with respect to a mechanical measurement in the structure. In this case, the water pressure during the permeability test was used. Load ratio was obtained based on the value of water pressure that was accompanied by the first AE burst, divided by the maximum pressure during the experiment. Calm ratio was calculated from AE hits during the unloading (reduction of water pressure) divided by the hits during the whole process of pressurization (JSNDI, 2000). Briefly, a healthier state is indicated by large Load ratios and low values of Calm ratio. Figure 7a shows the cumulative AE hits during the permeability test at -4 to -5 m in depth (cf. at -4.5 m in Fig. 6). For simplicity water pressure is normalized to its maximum value (0.5 MPa) on the horizontal axis, i.e. the Load ratio can be read from the horizontal value showing the onset of AE activity. In the case of Pier 1 before repair, AE started with a slight pressure of 6.2%, while after repair the onset of AE hits shifted to the larger value of 25.2%. In Pier 2, however, no remarkable change was obtained even after repair i.e., 25.5% before, to 29.5% after repair. These results lead to two important conclusions: (i) P1 was damaged but sufficiently reinforced. (ii) P2 was in acceptable damage state even before repair and a slight recovery was obtained afterward.

In Fig. 8a, AE activity of Pier 1 during both processes of water pressurization and its reduction is shown. Since the resulted Calm ratio of 0.11 before, increased to 0.35 after repair, recovery due to repair could not be assumed by the Calm ratio. For Pier 2, improvement after repair could not be obtained from Calm ratio, either (see Fig. 8b). However, the essential reduction of AE activity indicated simultaneous reduction of active sources.

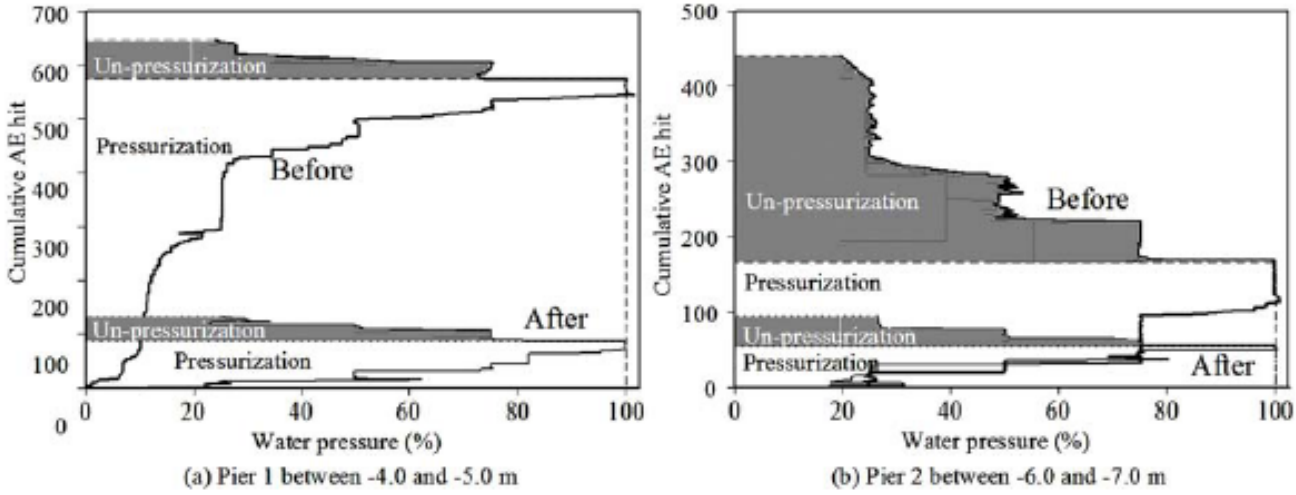

Fig. 8 AE hits activity during both of water pressurization and its reduction processes.

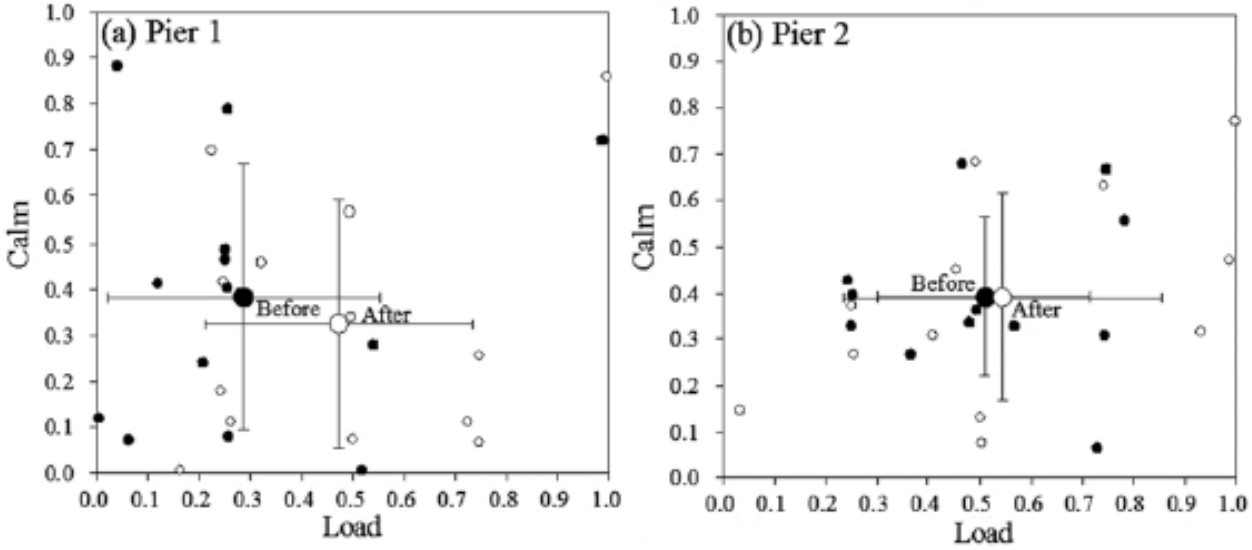

Fig. 9 Calm ratio and Load ratio based on ringdown count.

All derived ratios from both piers are plotted in Fig. 9. The small dots correspond to vertical zones of 1 m and are distributed over the chart; however, from the average of Load ratio a large difference appeared in Pier 1 between before and after, while only a slight difference was obtained in Pier 2. The figure also suggests that Calm ratio seems less sensitive to repair effect than Load ratio.

Discussion

Repair Effect from AE Hit Activity

From the AE activity of Pier 1, a large decrease of AE hits was found in deeper areas, and in those areas considerable quantity of grout was injected; For Pier 2, although the AE hits tended to decrease after repair, the decrease of hits was not as large as in Pier 1, and the quantity of grout did not correlate to the variation of AE activity, either. Here, it should be reminded that grouting in two directions was performed in Pier 1, whereas only in the horizontal direction for Pier 2. Furthermore the vertical grouting employed borehole of larger diameter than that of the horizontal, resulting in increased quantity of injected grout in Pier 1 (see the maximum value in Fig. 6) in comparison with Pier 2. Those all attributed to the difference in AE activity between Pier 1 and Pier 2, suggesting greater repair effect in Pier 1 than in Pier 2.

The number of AE hits after repair should also be discussed. Specifically in Pier 1, a steep change was obtained in the number of AE after repair, which stood at 602 and 348 at –9.0 and –12.0 m, respectively, while Pier 2 showed 133 hits at the maximum. This implies that although recovery rate was estimated to be small for Pier 2, it is healthier than Pier 1. Repair effect/recovery rate, and present health status should thus be considered from different points of view.

Repair Effect from AE Related Damage Indices

The above assumption can also be followed by AE related damage indices. As shown in Fig. 9, a large amount of increase in Load ratio was obtained in Pier 1 while only a slight increase in Pier 2. Thus, the recovery effect due to repair was obviously superior for Pier 1 than for Pier 2. However, from the point of view of soundness, Pier 2 was significantly healthier even from the original state (see the average before repair in Pier 2) and remained so despite the high recovery of Pier 1.

Quantification of Recovery Rate

Using AE related damage indices, current damage status of structures can be evaluated as described above; however, recovery rate, suggesting how much degree the structures were repaired, could not be quantified. Since both Calm ratio and Load ratio are relative values, normalized by an accumulated number of AE activity during the whole loading cycle or by the maximum value of referred parameter like pressure, respectively, these indices do not take into account substantial differences in the obtained number of AE hits before and after repair. As can be found in Fig. 8b and Fig. 9b, the number of AE hits decreased after repair, while the Calm ratio remained the same value even after repair as before. Therefore, we propose the recovery rate considering the numbers of AE hits obtained before and after repair.

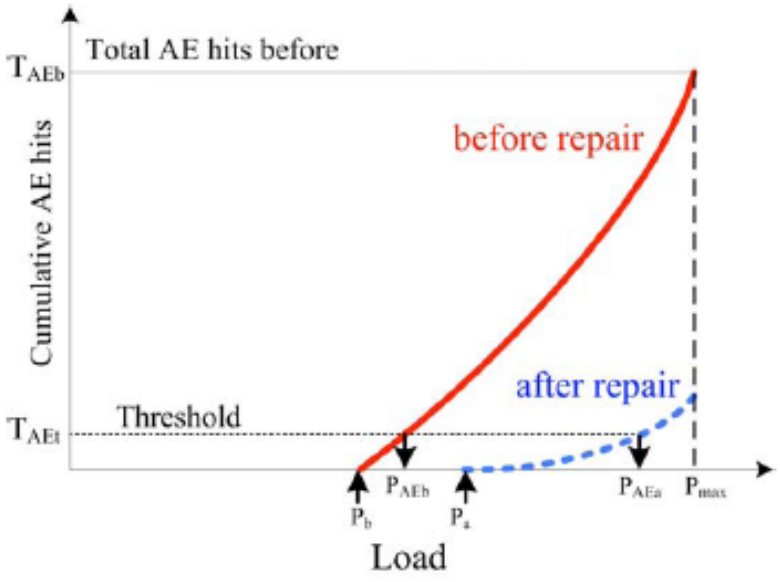

Fig. 10 Conceptual illustration of improved Load (i-Load) ratio.

Specifically for the recovery effect, Load and Calm ratios are modified based on the AE activity observed. The idea is demonstrated in Fig. 10 for the modification of Load ratio. Here, two typical AE hits vs. load curves (before and after repair) are shown. Conventional Load ratios are defined by dividing P_b, or P_a values (before and after repair) with the previous maximum load, P_{max}. Instead, we introduce the threshold value (in percent α) to determine the onset of cumulative AE curve. Suppose total AE hits before repair, T_{AEb}, is 100 and we set α to be 10%. Thus, the threshold hit value or T_{AEt} is 10. This defines P_{AEb} for AE hits vs. load curve before repair.

After the repair, we use the same threshold value as before, i.e., 10 in this case and we obtain P_{AEa}. By dividing P_{AEb} and P_{AEa} with the previous maximum load, P_{max}, we define *improved Load ratios* or "i-Load" ratios. We employ an identical condition for judging the onset of AE curves for before and after repair.

For modification of Calm ratio, we multiply a conventional Calm ratio with the ratio of cumulative AE activity after repair to that before repair. This allows us to factor in the variation of AE hits before and after. This new index is named *improved Calm ratio* or "i-Calm" ratio.

In reference to the AE activity data used in Fig. 9 and setting α as 10%, the i-Load and i-Calm ratios are obtained as shown in Fig. 11. In pier 1, the average coordinate shifted from (0.4, 0.33) before repair to the right bottom on the chart at (0.68, 0.03). This shift clearly indicates a high recovery rate after repair. Recovery can be also found in Pier 2 from (0.4, 0.4) to (0.52, 0.28), but not so dramatic as in Pier 1. As shown in Fig. 9, Calm ratio did not reflect the repaired condition effectively, as almost identical values were obtained before and after. By considering the number of AE hits, we can account for the recovery of the structure due to repair with the use of i-Calm ratio. It is noted that the use of α = 5% results in the same trend as in 10%, suggesting the proper range of α in this case being 5 to 10%; however, to determine the appropriate value for other structures, further studies are necessary.

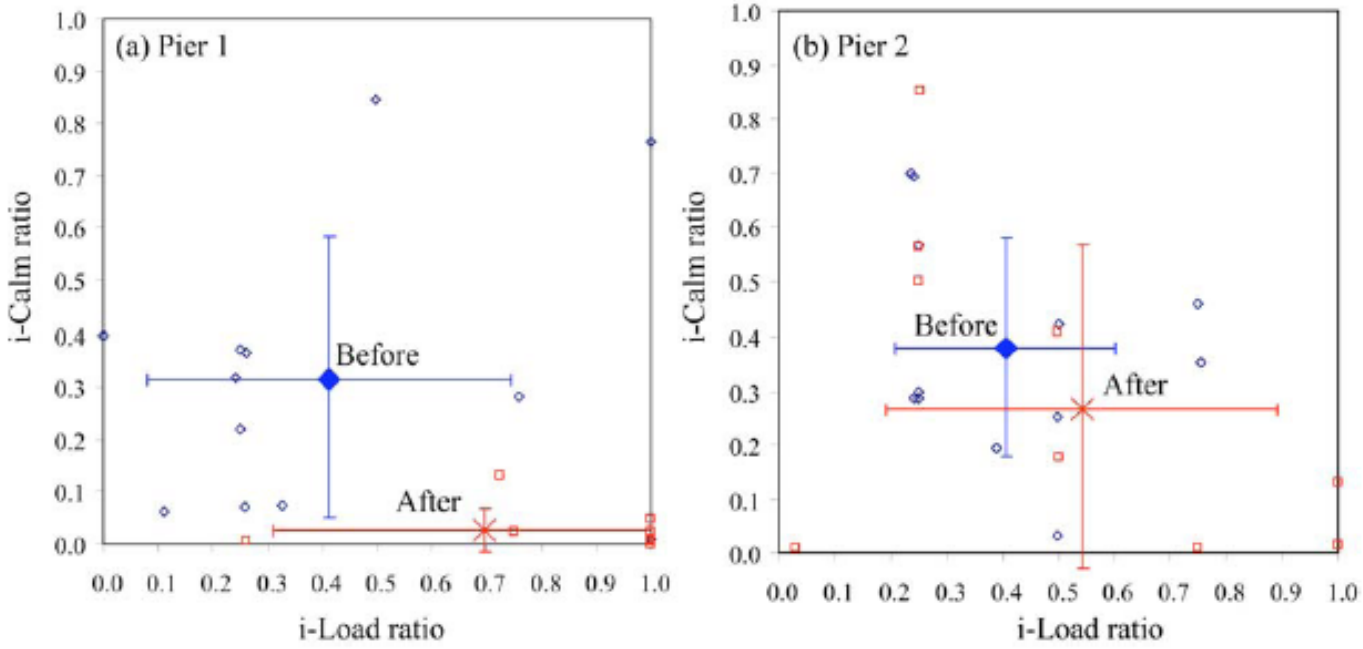

Fig. 11 Improved Calm (i-Calm) ratio and improved Load (i-Load) ratio to assess the recovery rate.

Conclusion

In this paper, two NDT techniques, namely seismic tomography and AE technique, are applied in order to evaluate the improvement after repair in severely deteriorated large concrete piers. Pier 1 was repaired well with a large amount of grout injection in the vertical and lateral direction, while a less volume of grout was filled in Pier 2. Contrary to the general assumption, a substantial velocity decrease was found in Pier 1, owing to the resultant low mechanical properties of the freshly injected grout that is assisted by scattering effect. With hardened grout properties, velocity values are further estimated, resulting in velocity increases. Discrepancies of AE activity before and after repair indicated the repair effectiveness, specifically with employing

damage indices of Calm and Load ratios. Additionally in order to quantify the recovery rate improved Calm and improved Load ratios are newly defined, with the consideration of the number of AE hits, and a lowered AE activity in the structure due to repair.

References

Aggelis, D. G. and Shiotani, T. (2006a), "Wave behavior of concrete structures repaired by cement injection", submitted.

Aggelis, D. G. and Shiotani, T. (2006b), "Damage Evaluation on Concrete Materials Using Characteristics of Elastic waves", *Proc. of Structural Faults and Repair 2006*, Edinburgh, 13-15 June, (in CD).

Chaix, J. F., Garnier, V., and Corneloup, G. (2006), "Ultrasonic wave propagation in heterogeneous solid media: Theoretical analysis and experimental validation", Ultrasonics, **44**, 200-210.

Kobayashi, Y., Shiojiri, H. and Shiotani, T. (2006), "Damage Identification Using Seismic Travel Time Tomography on the Basis of Evolutional Wave Velocity Distribution Model", *Proc. of Structural Faults and Repair 2006*, Edinburgh, 13-15 June, (in CD).

Luo, X., Haya, H., Inaba, T., Shiotani, T., and Nakanishi, Y. (2004), "Damage Evaluation of Railway Structures by Using Train-Induced AE", Construction and Building Materials, **18**(3), 215-223.

M. J. Sansalone, and W. B. Streett (1997), *Impact-Echo, Nondestructive Evaluation of Concrete and Masonry*, Bullbrier Press, Ithaca, N.Y.

Shiotani, T., Nakanishi, Y., Iwaki, K., Luo, X. and Haya, H. (2005a), "Evaluation of Reinforcement in Damaged Railway Concrete Piers by Means of Acoustic Emission", Journal of Acoustic Emission, **23**, 260-271.

Shiotani, T., Luo, X., Haya, H. and Ohtsu, M. (2005b), "Damage Quantification for Concrete Structures by Improved *b*-Value Analysis of AE", *11th International Conference on Fracture*, CD-ROM.

Shiotani, T. and Aggelis, D. G. (2006), "Damage Quantification of Aging Concrete Structures by Means of NDT", *Proc. of Structural Faults and Repair 2006*, Edinburgh, 13-15 June, (in CD).

The Japanese Society for Non-Destructive Inspection (2000), "Recommended Practice for In Situ Monitoring of Concrete Structures by Acoustic Emission", NDIS2421. JSNDI, Japan.

Tsinopoulos, S. V., Verbis, J. T., Polyzos, D. (2000), "An iterative effective medium approximation for wave dispersion and attenuation predictions in particulate composites", Adv. Composite Lett., **9**, 193–200.

Waterman, P.C., Truell, R. (1961), "Multiple scattering of waves", J. Math. Phys., **2**, 512–537.

Ying, C.F., Truell, R. (1956), "Scattering of a plane longitudinal wave by a spherical obstacle in an isotropically elastic solid", J. Appl. Phys. **27**, 1086–1097.